

The effect of flaw shape on fracture initiation at a blunt flaw

E. Smith

Received: 2 June 2004 / Accepted: 15 September 2006 / Published online: 20 December 2006
© Springer Science+Business Media, LLC 2006

Abstract The author is involved in a wide-ranging research programme, the objective being to extend the fracture mechanics methodology for sharp cracks to blunt flaws, so as to take credit for the blunt flaw geometry. The approach is based on the cohesive process zone representation of the micro-mechanistic processes that are associated with fracture. An earlier paper has derived a blunt flaw fracture initiation relation which gives the critical elastic flow-tip peak stress σ_{per} (a “signifier” of a critical condition in the process zone) in terms of the process zone material parameters, subject to the proviso that the process zone size s is small compared with the flaw depth (length) and any characteristic dimension other than the flaw root radius ρ . The relation has been derived using a “two-extremes” procedure, whereby the separate σ_{per} solutions for small and large s/ρ are blended together to give an all-embracing relation that is valid for all s/ρ . A key feature of the relation is that σ_{per} essentially depends on only one geometrical parameter: the flaw root radius ρ . Though the relation has evolved from a consideration of the characteristics of one model, i.e. that of an elliptical flaw in an infinite solid that is subjected to an applied tensile stress, it is anticipated that the relation can be applied equally well for a wide range of geometrical configurations involving different flaw shapes. It is against this background that the present paper demonstrates that

the relation also applies to the behaviour of an intrusion type flaw in the surface of a semi-infinite solid subjected to an applied tensile stress.

Introduction

Linear elastic fracture mechanics (LEFM) of cracks is now well-established, and is based on the stress field in the immediate vicinity of a crack tip being described by the stress intensity factor K , with crack extension occurring when K is equal to a critical value K_c , which is referred to as the fracture toughness of the material. This methodology has been applied to a wide range of situations that are characterised by the micro-mechanistic processes, which lead to fracture, being confined to a small region in the vicinity of a crack tip. K_c is a “signifier” of a critical condition near the crack tip.

However, there are many engineering situations that involve flaws or notches that are blunt rather than being crack-like or sharp, and for such blunt flaws it is overly conservative to treat them as cracks and use LEFM methods. This is the case, for example with stress concentrations that are design features, and with bore-holes and excavations in geological structures. Another example is Delayed Hydride Cracking (DHC) initiation at the tip of a blunt debris fretting flaw in CANDU (CANada Deuterium Uranium) nuclear reactor Zr–2.5 Nb alloy pressure tube material [1]. It is this latter case that has provided the motivation to extend the fracture mechanics methodology for sharp cracks to blunt flaws, so as to take credit for the blunt flaw geometry in structural integrity assessments.

E. Smith (✉)
School of Materials, Manchester University, Grosvenor
Street, Manchester M1 7HS, UK
e-mail: ted.smith14@btopenworld.com

The strategy has been to parallel, as far as possible, the methods that have been developed for cracks. This means that the approach has been based on the cohesive process zone representation of the non-linear processes that are associated with fracture, whereby the non-linearity is modelled so that it is confined to an infinitesimally thin strip. This type of representation has been used to describe stress relaxation due to plasticity at a stress concentration, where the process zone is often referred to as a strip yield zone [2–4]. It has also been applied to many other situations including microcracking in concrete, rocks and many other ceramic-type materials [5].

An earlier paper [6] has derived a blunt flaw fracture initiation relation which gives the critical elastic flaw-tip peak stress σ_{pcr} (analogous to K_{c} for a sharp crack) in terms of the process zone material parameters, subject to the proviso that the process zone size s is small compared with the flaw depth (length) and any other characteristic dimension other than the flaw root radius ρ . The relation has been derived using a “two-extremes” procedure, whereby the separate solutions for small and large s/ρ are blended to give an all-embracing relation that is valid for all s/ρ , a key feature of the relation being that σ_{pcr} essentially depends on only one geometrical parameter, namely the flaw root radius ρ . Though the relation has evolved from a consideration of the characteristics of one model, i.e. that of an elliptical flaw in an infinite solid that is subjected to an applied tensile stress, it is anticipated that the relation can be applied equally well for a wide range of geometrical configurations involving different flaw shapes. It is against this background that the present paper demonstrates that the relation also applies to the behaviour of an intrusion type flaw in the surface of a semi-infinite solid that is subjected to an applied tensile stress.

The process zone approach

Figure 1 shows a general Mode I two-dimensional flaw with a radius of curvature ρ , that is in a solid which is

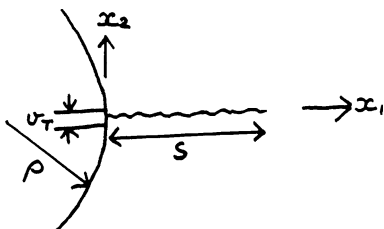


Fig. 1 Process zone of length s in the immediate vicinity of a flaw root with radius of curvature ρ

subjected to an applied nominal stress, and has a process zone of length s emanating from the flaw root. The process zone is an infinitesimally thin strip within which the restraining tensile stress is assumed to have a uniform value p_c . This is the classic Dugdale–Bilby–Cottrell–Swinden (DBCS) [2, 3] representation, with the stress uniformity assumption simplifying the considerations considerably. The relative displacement across the process zone at the flaw surface is v_T , and it is assumed that fracture initiates when v_T attains a critical value v_c , a “signifier” of a critical condition in the process zone. The material parameters p_c and v_c are key inputs into the process zone methodology, and provide the essential link between the methodology and the mechanisms that are operative at the microstructural level. The process zone size s is determined by recognising that the stress must be finite at the leading edge of the process zone.

The values of p_c and v_c are assumed to be flaw geometry independent, and consequently the values for a blunt flaw are assumed to be the same as for a sharp crack. With Mode I deformation, when the methodology is applied to a long crack where the process zone length s is small compared with the crack length and any other geometrical dimension such as the remaining ligament width, the DBCS representation gives

$$v_c = \frac{K_{\text{IC}}^2}{E_0 p_c} \quad (1)$$

where K_{IC} is the Mode I fracture toughness of the material, and $E_0 = E/(1-\nu^2)$ where E is Young’s modulus and ν is Poisson’s ratio for the material outside the process zone, with the material being assumed to behave elastically.

The two-extremes procedure

As indicated in the Introduction, the two-extremes procedure [6] derives a blunt flaw fracture initiation relation which gives the critical elastic flaw-tip peak stress σ_{pcr} , subject to the proviso that the process zone size s is small compared with the flaw depth (length) and any other characteristic dimension other than the flaw root radius ρ . The relation is derived by blending the separate σ_{pcr} solutions for small and large s/ρ to give an all-embracing relation that is valid for all s/ρ .

In addressing the small s/ρ situation, let us consider the Mode I model where there is a uniform stress (p_c) process zone emanating from the planar surface of a semi-infinite solid (Fig. 2). It is assumed that the tensile

stress $\sigma(x)$ along the plane $x_2 = 0$ in the absence of the process zone is given by the relation

$$\sigma(x) = \sigma_p \left(1 - \frac{x}{h}\right) \tag{2}$$

where x is measured from $x_1 = 0$ along the x_1 axis. This stress simulates the tensile stress in the immediate vicinity of the root of a flaw with σ_p being the peak tensile stress at the flaw surface while h is a length parameter, which is a measure of the stress gradient at the flaw root. The results of Tada et al. [7] have been used [6, 8], in conjunction with the methodology described in the preceding section, to give the critical elastic flaw-tip peak stress σ_{pcr} required for fracture initiation as

$$\frac{\sigma_{\text{pcr}}}{p_c} = 1 + \frac{0.81K_{\text{IC}}}{p_c(\pi h)^{1/2}} \tag{3}$$

this relation being applicable for any flaw provided that the process zone length s is small compared with h , which corresponds to $K_{\text{IC}}/p_c h^{1/2}$ being small.

In applying relation (3) to the model of a two-dimensional elliptical notch of root radius ρ and length $2a$ in an infinite solid that is subjected to an applied nominal tensile stress σ_n (Fig. 3), we note that the parameter h for this elliptical notch is given by the expression [9]

$$h = \frac{\rho}{2} \left\{1 + \frac{1}{2} \left(\frac{\rho}{a}\right)^{1/2}\right\} / \left\{1 + \frac{3}{4} \left(\frac{\rho}{a}\right)^{1/2}\right\} \tag{4}$$

an expression which checks with the well known solution [10] for a circular hole, i.e. $h = 3a/7$ when $\rho = a$. If we focus attention on flaws for which $0 < \rho/a < 1$, i.e. those which are sharper than a circular hole, then expressions (3) and (4) allow the critical failure stress σ_{pcr} to be given by the relation

$$\frac{\sigma_{\text{pcr}}}{p_c} = 1 + \frac{\lambda K_{\text{IC}}}{p_c(\pi\rho)^{1/2}} \tag{5}$$

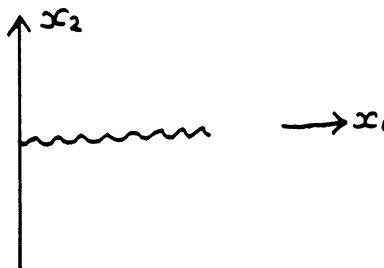


Fig. 2 The planar surface model

where

$$\lambda = 0.81(\rho/h)^{1/2} \tag{6}$$

is weakly dependent on the ratio ρ/a , i.e. it varies between 1.14 for a very sharp flaw ($\rho/a \rightarrow 0$) when the near-tip flaw profile becomes parabolic, and 1.24 for a circular flaw ($\rho/a = 1$). Noting relation (4) and the qualification with regards to the viability of relation (3), it follows that relation (5) is applicable provided that the process zone length s is small compared with ρ , which corresponds to $K_{\text{IC}}/p_c \rho^{1/2}$ being small.

Now let us proceed to the other extreme, where the process zone size is large compared with ρ , i.e. $K_{\text{IC}}/p_c \rho^{1/2}$ is large, though is still small compared with the flaw depth (length). In this case, the effective stress intensity factor K_I required for fracture initiation must equal K_{IC} . But $K_{\text{IC}} = \sigma_n(\pi a)^{1/2}$ with $\sigma_{\text{pcr}}/\sigma_n = K_I = 1 + 2(a/\rho)^{1/2}$ for the elliptical flaw model (Fig. 3), where K_I is the elastic stress concentration factor and it therefore follows that

$$\frac{\sigma_{\text{pcr}}}{p_c} = \frac{2K_{\text{IC}}}{p_c(\pi\rho)^{1/2}} \tag{7}$$

as $\rho \rightarrow 0$. This relation is strictly valid only for the elliptical flaw model, and for other flaw configurations, relation (7) is replaced by the more general relation

$$\frac{\sigma_{\text{pcr}}}{p_c} = \frac{\mu K_{\text{IC}}}{p_c(\pi\rho)^{1/2}} \tag{8}$$

where μ is given by the expression

$$\mu = \frac{\sigma_p(\pi\rho)^{1/2}}{K_I} \tag{9}$$

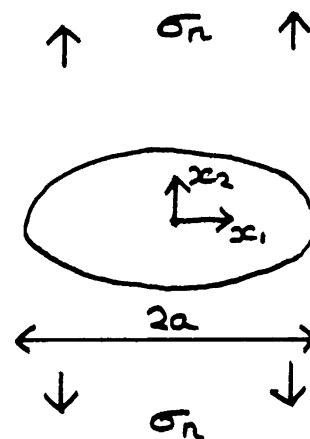


Fig. 3 Model of an elliptical flaw in an infinite solid subjected to an applied nominal tensile stress $\sigma_{22} = \sigma_n$

in the limit as $\rho \rightarrow 0$, where σ_p is the peak stress at the flaw root and K_I is the stress intensity factor in the limiting situation; μ is of course equal to two for the elliptical flaw model.

With $\theta = K_{IC}/p_c(\pi\rho)^{1/2}$, relation (5) for the small s/ρ situation and relation (8) for the large s/ρ situation can be written respectively as

$$\frac{\sigma_{\text{pcr}}}{p_c} = 1 + \lambda\theta \quad (\text{small}\theta) \quad (10)$$

and

$$\frac{\sigma_{\text{pcr}}}{p_c} = \mu\theta \quad (\text{large}\theta) \quad (11)$$

with λ being given by relation (6) and μ being given by relation (9). These relations are applicable to a general flaw, not necessarily an elliptical flaw, subject of course to the proviso that the process zone is small compared with the flaw length (depth) or any other characteristic length, such as remaining ligament width. The simplest functional relation that satisfies both relations (10) and (11) is

$$\frac{\sigma_{\text{pcr}}}{p_c} = 1 + \frac{\theta(\lambda + \mu\theta)}{(1 + \theta)} \quad (12)$$

This is a simple expression that is exact for both small and large θ and we assume that it is reasonably accurate for intermediate θ values. The reasonableness of this assumption has been tested by appealing to the analytical results for the analogous Mode III elliptical flaw model [1, 8]. In this case $\mu = 1$ and $\lambda = 1$, irrespective of the value of ρ/a , and the resulting σ_{pcr} expression is in fact exact for intermediate θ values. The author (unpublished work) has also tested the assumption against the analytical results for the Mode III key-hole model, albeit for the limiting case where ρ/a is vanishingly small (a is the flaw depth and ρ the hole radius). In this case $\mu = 2^{1/2}$ and $\lambda = 1$ and the resulting σ_{pcr} expression is in very close agreement with the exact results for intermediate θ values. In the light of these accords it is reasonable to assume that relation (12) is reasonably accurate when applied to Mode I scenarios for intermediate θ values, as well as small and large θ values.

Returning to the elliptical flaw model (Fig. 3), we remember (see the comments following relation (6)) that the parameter λ only varies between 1.14 ($\rho/a \rightarrow 0$) and 1.24 ($\rho/a = 1$) while $\mu = 2$. Inspection of relation (12) shows that if we input $\lambda = 1.14$ and $\mu = 2$, then the resulting relation

$$\frac{\sigma_{\text{pcr}}}{p_c} = 1 + \frac{\theta(1.14 + 2\theta)}{(1 + \theta)} \quad (13)$$

approximates to relation (12) to within 2%. Relation (13) is an improvement upon a Mode I simplified relation suggested earlier [1, 8]. This relation was

$$\frac{\sigma_{\text{pcr}}}{p_c} = 1 + 2\theta \quad (14)$$

which satisfies the large θ condition (see relation (11)) and the condition that $\sigma_{\text{pcr}}/p_c = 1$ when $\theta = 0$, but it does not satisfy the small θ condition (see relation (10)).

Support for the viability of relation (13) is provided by the numerical results of Vitek [11]. He analysed the (Mode I) model in Fig. 3 by representing the displacement discontinuity across the process zones at the notch roots by discrete dislocations, and reducing the problem to the solution of a system of linear equations. Then, albeit guided by the analogous Mode III analytical solution [4], he constructed an empirical formula which approximately fitted the numerical results. As indicated in earlier work [1, 8], for the case where the flaw root radius and the process zone length are both small compared with the flaw length, his approximate empirical formula was equivalent to relation (14) and thus very close to relation (13).

Relation (12) is quite general and gives σ_{pcr} provided we know the values of the parameters λ and μ , which can be obtained from respectively relations (6) and (9), which depend respectively on a knowledge of the local stress distribution in the immediate vicinity of the flaw root (which gives the parameter h), and the σ_p - K_I relation for the flaw in question. However, it would be far easier if we could simply use relation (13) which, as it stands, strictly refers to the model of an elliptical flaw in an infinite solid for the limiting case where the flaw is sharp ($\rho/a \rightarrow 0$) and the flaw root profile is parabolic. In other words, we pose the question as to whether relation (13) applies more generally to other Mode I situations, albeit in an approximate sense, subject of course to the proviso that we are dealing with reasonably sharp flaws ($\rho/a < 1$) and situations where the process zone is small in comparison with the flaw depth (length). This requires that the parameter h and the σ_p - K_I relation (i.e. the parameter μ) are approximately dependent only on ρ and not on other geometrical parameters. (This is clearly not the case with Mode III situations where $\mu = 1$ for an elliptical flaw and $2^{1/2}$ for a key-hole flaw). However, we believe that with Mode I deformation, the parameter h and the σ_p - K_I relation are

approximately dependent only on ρ , and therefore that relation (13) is applicable, to a reasonable degree of accuracy, for a wide range of geometrical configurations, including the case of a semi-elliptical flaw in the surface of a semi-infinite solid. An objective of the author’s research is, if possible, to support this view. It is against this background that the next section presents an analysis of the behaviour of an intrusion type flaw in the surface of a semi-infinite solid that is subjected to an applied tensile stress.

Intrusion type flaw analysis

Figure 4 shows schematically an edge-type intrusion flaw (not a flaw with an elliptical profile) in the surface of a semi-infinite solid that is subjected to an applied tensile stress σ_n . The flaw has a depth a and root radius ρ , with the profile being defined by the relation

$$\frac{\bar{y}}{a} = \left(\frac{\bar{x}}{a}\right)^{1/2} \left[\frac{\bar{x}}{a} + \left(\frac{2\rho}{a}\right)^{1/2} \right] / \left[1 - \frac{\bar{x}}{a} \right]^{1/2} \tag{15}$$

With this relation, $\bar{y} \rightarrow \infty$ as $\bar{x} \rightarrow a$. Zheng [12] has provided an expression which gives the tensile stress $\sigma(x)$ at a distance x ahead of the flaw root. This expression is

$$\frac{\sigma(x)}{\sigma_n} = \frac{[-(2\alpha - a)\psi^6 + 3\alpha a(2\alpha - a)\psi^4 - 4\alpha^3 a\psi^3 + 3\alpha^3 a^2\psi^2 - \alpha^4 a^3]}{(-\psi^2 + \alpha a)^3(2\alpha - a)} \tag{16}$$

where the parameters ψ and α are related to the flaw depth a , flaw root radius ρ and distance x via the relations

$$2\psi = (\alpha + a + x) + [(\alpha + a + x)^2 - 4\alpha a]^{1/2} \tag{17}$$

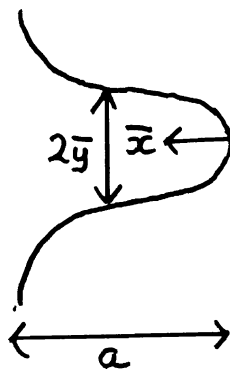


Fig. 4 An intrusion type flaw

and

$$\frac{\alpha}{a} = 1 + \left(\frac{2\rho}{a}\right)^{1/2} \tag{18}$$

With $\psi/a = \phi$ and $\alpha/a = \chi$, expression (16) can be written in the form

$$\frac{\sigma(x)}{\sigma_n} = \frac{[-(2\chi - 1)\phi^6 + 3\chi(2\chi - 1)\phi^4 - 4\chi^3\phi^3 + 3\chi^3\phi^2 - \chi^4]}{(-\phi^2 + \chi)^3(2\chi - 1)} \tag{19}$$

while relation (17) can be written in the form

$$2\phi = 1 + \chi + \frac{x}{a} + \left[\left(1 + \chi + \frac{x}{a}\right)^2 - 4\chi \right]^{1/2} \tag{20}$$

Since we are interested in the behaviour of sharp flaws for which ρ/a is not large, then provided that ρ is not zero, relations (18) and (20) show that

$$\phi \equiv \chi + w \tag{21}$$

with

$$w = \frac{\chi x}{a(\chi - 1)} \tag{22}$$

whereupon w is small. Relations (18), (19), (21) and (22) then show that

$$\sigma(x) = \sigma_p \left(1 - \frac{x}{h}\right) \tag{23}$$

with the peak stress σ_p , i.e. the value of $\sigma(x)$ when $x = 0$, being given by the relation

$$\frac{\sigma_p}{\sigma_n} = K_t = \frac{\left[1 + \left(\frac{2\rho}{a}\right)^{1/2}\right] \left[3 + 2\left(\frac{2\rho}{a}\right)^{1/2}\right]}{\left(\frac{2\rho}{a}\right)^{1/2} \left[1 + 2\left(\frac{2\rho}{a}\right)^{1/2}\right]} \tag{24}$$

where K_t is the flaw tip stress concentration factor, while the parameter h is given by the relation

$$h = \frac{\rho}{2} \left[1 + \frac{2}{3} \left(\frac{2\rho}{a}\right)^{1/2} \right] / \left[1 + \left(\frac{2\rho}{a}\right)^{1/2} \right] \tag{25}$$

This result compares with relation (4) for an elliptical flaw in an infinite solid. It follows from relations (6) and (25) that the parameter λ is given by the relation

$$\lambda = 0.81 \left[2 \left\{ 1 + \left(\frac{2\rho}{a} \right)^{1/2} \right\} \right]^{1/2} / \left[1 + \frac{2}{3} \left(\frac{2\rho}{a} \right)^{1/2} \right]^{1/2} \quad (26)$$

In determining the crack tip stress intensity factor K_I for the limiting case where $\rho = 0$ and the flaw degenerates into a (tapered) crack, with K_I being defined in accord with the relation

$$\sigma(x) = \frac{K_I}{(2\pi x)^{1/2}} \quad (27)$$

Zheng [12] has shown that

$$K_I = \frac{3}{4} (2\pi a)^{1/2} \sigma_n \quad (28)$$

a relation that can be obtained from relations (19) and (20) noting that relation (18) gives $\chi = \alpha/a = 1$. Since relation (24) gives

$$\frac{\sigma_p}{\sigma_n} = 3 \left(\frac{a}{2\rho} \right)^{1/2} \quad (29)$$

in the limit as $\rho \rightarrow 0$, it follows from relations (9), (28) and (29) that the parameter μ is equal to 2.

Relation (26) shows that the parameter λ is weakly dependent on the ratio ρ/a , in that it only varies between 1.14 and 1.25 as ρ/a varies between zero and 0.5. With the elliptical flaw (see the comments preceding relation (13)); λ only varies between 1.14 and 1.24 as ρ/a varies between zero and 1.0. Furthermore the value of μ , i.e. 2, is the same for both the elliptical and intrusion type flaw. In the light of these similarities, it may be concluded that relation (13), as well as applying to an elliptical flaw, also applies approximately to an intrusion type flaw over a wide range of intrusion flaw geometries.

Discussion

Motivated by the technological problem [1] of DHC at the tip of a blunt debris fretting flaw in CANDU nuclear reactor Zr–2.5 Nb alloy pressure tube material, the author is involved in a wide-ranging research programme, whose objective is to extend the fracture mechanics methodology for sharp cracks to blunt flaws, so as to take credit for the blunt flaw geometry. The approach is based on the cohesive process zone representation of the micro-mechanistic processes that are associated with fracture. The considerations have

been focussed primarily on situations where the process zone size is small compared with the flaw size and with relatively sharp flaws for which $\rho/a \ll 1$, ρ being the flaw root radius of curvature and a being the flaw size. The main concern is with regard to Mode I loading scenarios, although extensive use has been made of Mode III simulation models to provide a guide as to how to proceed with Mode I analyses. A key objective has been to find a parameter, analogous to the stress intensity factor K for a sharp crack, to quantify fracture initiation; this parameter is the elastic flaw tip peak stress σ_p with initiation occurring when σ_p attains a critical value σ_{per} which is analogous to K_{IC} for a sharp crack.

In general the stress distribution in the vicinity of a flaw root depends on σ_p , ρ and other geometrical parameters as shown, for example, by the elliptical flaw results (see Eqs. (2) and (4)), although it depends approximately on only σ_p and ρ within restricted ranges of geometrical configurations, a point that has been recognised by other workers, for example Glinka and Newport [13]. It is intuitively reasonable, therefore, to expect a similar behaviour pattern as regards fracture initiation. The author has derived a fracture initiation relation using a “two-extremes” procedure, whereby the separate solutions for small and large s/ρ (s is the process zone size) are blended together to give an all-embracing relation that is valid for all s/ρ . In general this relation depends on other geometrical parameters other than the flaw root radius ρ (see relation (12) where the parameters λ and μ are in general geometry dependent) but the elliptical flaw results in Section “The two-extremes procedure” show (see relation (13)) that, within restricted ranges of flaw geometries, i.e. for sharp flaws, σ_{per} depends, to a high degree of accuracy, only on the process zone material parameters K_{IC} and p_c via the parameter $\theta = K_{IC}/p_c(\pi \rho)^{1/2}$ and the flaw root radius ρ . The important conclusion that arises from the work in this paper (see Section “Intrusion type flaw analysis”) is the demonstration that relation (13) is also approximately applicable to the behaviour of an intrusion type flaw in the surface of a semi-infinite solid that is subjected to an applied tensile stress.

Further support for the wide-ranging applicability of relation (13) is provided by a comparison of its predictions with those obtained by a numerical engineering procedure [1] that has been developed in the context of the DHC problem. This procedure consists of the following steps: (1) a cubic polynomial equation is fitted to the elastic flaw tip stress distribution using the least squares method; (2) generalised closed form equations for the stress intensity factor and crack

Table 1 Critical peak stress (σ_{per}) values

Flaw root radius ρ (mm)	σ_{per} (MPa)	
	Engineering procedure	Relation (13)
0.050	960	996
0.100	790	818
0.150	720	742
0.200	680	698
0.250	655	669
0.300	635	648
0.350	620	632
0.400	610	618
0.450	600	608
0.500	590	599

mouth opening displacement for cracks emanating from the tips of blunt flaws for a wide range of flaw geometries have been developed; (3) these generalised equations have been incorporated into a closed form process zone model, based on the cubic polynomial stress distribution, to calculate the process zone displacement at the flaw surface; (4) the equations of step (3) are re-arranged to give the flaw tip peak stress σ_{per} needed for fracture initiation. The numerical engineering procedure has been applied [6] to 45°-V flaws with finite root radius, while allowing for a finite width (4 mm) of the configuration. Calculations were performed for flaw depths of 0.25, 0.50, 0.75 and 1.0 mm, with appropriate input values of K_{IC} (in the context of this paper's terminology) = 4.5 MPa $\sqrt{\text{m}}$ and $p_c = 450$ MPa. $K_{\text{IC}} \equiv K_{\text{IH}}$, the threshold stress intensity for the extension of a sharp crack via the DHC mechanism. The dependence of σ_{per} on flaw depth was 2% or less, which is consistent with relation (13) which exhibits no depth dependency. The results are shown in Table 1, which also includes results obtained by use of relation (13) noting that $\theta = K_{\text{IC}}/p_c(\pi\rho)^{1/2}$. The agreement between the two sets of results is very good, which provides support for the wide-ranging applicability of relation (13).

Before concluding this discussion it is important to mention that although relation (13) involves only one geometrical parameter: the flaw root radius of curvature ρ through the parameter $\theta = K_{\text{IC}}/p_c(\pi\rho)^{1/2}$, this

does not mean that other geometrical parameters, for example flaw depth a , do not enter into the considerations. They do, by virtue of the fact that the nominal stress σ_n required for fracture initiation is equal to σ_{per}/K_t where K_t is the flaw tip stress concentration factor which increases with flaw depth for a fixed ρ .

Conclusion

The paper, by analysing the behaviour of an intrusion type flaw has provided further evidence to support a simple relation that quantifies fracture initiation at the root of a blunt flaw.

References

1. Scarth DA, Smith E (2001) J Pressure Vessel Technol 123:41
2. Dugdale DS (1960) J Mech Phys Solids 8:100
3. Bilby BA, Cottrell AH, Swinden KH (1963) The spread of plastic yield from a notch. Proceedings, Royal Society of London, A-272 p 304
4. Smith E (1967) Fracture initiation at a sharp notch. Proceedings, Royal Society of London, A-299 p 455
5. Fracture of Brittle, Disordered Materials: Concrete, Rock and Ceramics (1993) In: Baker G, Karihaloo BL (eds) Proceedings of IUTAM Symposium, September 20–24. The University of Queensland, Brisbane, Australia, published by E. and F.N. Spon (Chapman and Hall), London, UK
6. Smith E, Scarth DA (2002) Fracture mechanics of blunt notches. In: Soboyejo WO, Lewandowski JJ, Ritchie RO (eds) Mechanisms and mechanics of fracture, The John Knott Symposium. TMS, October 7–10, Columbus, OH, USA, p 71
7. Tada H, Paris PC, Irwin GR (1973) The stress analysis of cracks handbook. Del Research Corporation, Hellertown, PA, USA
8. Smith E, Scarth DA (2001) Extending fracture mechanics for cracks to the behaviour of notches. Proceedings of the 2001 ASME Pressure Vessels and Piping Conference, PVP-Vol 423, Atlanta, GA, USA, p 11
9. Smith E (1998) J Mater Sci 33:29
10. Knott JF (1973) Fundamentals of fracture mechanics. Butterworths, London, UK
11. Vitek V (1975) J Mech Phys Solids 24:67
12. Zheng H (1996) A study of the criterion for cracking of inhomogeneous inclusions. Ph.D. Thesis, University of Waterloo, Ontario, Canada
13. Glinka G, Newport A (1987) Int J Fatigue 9:143